energies

MDPI

Article

An Analytical Model for Wind Turbine Wakes under Pressure Gradient

Arslan Salim Dar and Fernando Porté-Agel *

Wind Engineering and Renewable Energy Laboratory (WIRE), École Polytechnique Fédérale de Lausanne (EPFL), 1015 Lausanne, Switzerland; arslan.dar@epfl.ch

* Correspondence: fernando.porte-agel@epfl.ch

Abstract: In this study, we present an analytical modeling framework for wind turbine wakes under an arbitrary pressure gradient imposed by the base flow. The model is based on the conservation of the streamwise momentum and self-similarity of the wake velocity deficit. It builds on the model proposed by Shamsoddin and Porté-Agel, which only accounted for the imposed pressure gradient in the far wake. The effect of the imposed pressure gradient on the near wake velocity is estimated by using Bernoulli's equation. Using the estimated near wake velocity as the starting point, the model then solves an ordinary differential equation to compute the streamwise evolution of the maximum velocity deficit in the turbine far wake. The model is validated against experimental data of wind turbine wakes on escarpments of varying geometries. In addition, a comparison is performed with a pressure gradient model which only accounts for the imposed pressure gradient in the far wake, and with a model that does not account for any imposed pressure gradient. The new model is observed to agree well with the experimental data, and it outperforms the other two models tested in the study for all escarpment cases.

Keywords: wakes; wind turbines; pressure gradient; analytical modeling

Citation: Dar, A.S.; Porté-Agel, F. An Analytical Model for Wind Turbine Wakes under Pressure Gradient. *Energies* **2022**, *15*, 5345. https://doi.org/10.3390/en15155345

Academic Editors: Majid Bastankhah, Ervin Bossanyi and Dries Allaerts

Received: 21 June 2022
Accepted: 14 July 2022
Published: 23 July 2022

1. Introduction

Wind turbine wakes can result in significant power losses within a wind farm, as they reduce the power available to the downwind turbines, as well as enhance the fluctuating loads experienced by these turbines [1]. Understanding and predicting these wakes is crucial, especially during the planning and layout optimization phase of a wind farm. Computationally inexpensive analytical tools are widely popular in the wind energy community for this purpose, as they offer fast and reasonably accurate estimations of wind turbine wakes, which enables testing different layout configurations and wind conditions in a relatively short time. Given their paramount importance, a number of analytical models for wind turbine wakes have been proposed over the years.

Most attempts to analytically model wind turbine wakes assume an underlying flat homogeneous terrain, which implies a zero pressure gradient situation. Early attempts at analytical modeling of wind turbine wakes started with Jensen [2], who applied mass conservation downwind of the turbine and assumed a top-hat distribution of the velocity deficit. Later, Frandsen et al. [3] used mass and momentum conservation around a wind turbine to estimate the velocity deficit in the wake. Similar to Jensen [2], they also assumed a top-hat distribution of the velocity deficit across the rotor cross-section. Based on the empirical evidence of a self-similar Gaussian distribution of velocity deficit in the turbine wake, Bastankhah and Porté-Agel [4] proposed an analytical model for the wake velocity deficit derived from streamwise mass and momentum conservation. Their model has since been adapted to different scenarios, such as wakes of turbines under yawed conditions [5], or the ones experiencing wind veer effects [6]. Recent advances in the analytical modeling of wakes include the so-called super-Gaussian model, which transitions from a top-hat

profile in the turbine near wake to a Gaussian profile in the far wake [7], a model for the wake velocity and added turbulence intensity based on a combination of analytical and numerical studies [8], analytical models for yawed turbine wakes [9] and for added streamwise turbulence intensity in the wake [10].

It is highly likely that wind turbines sited in complex flow conditions, such as heterogeneous surface roughness conditions or topographies, experience a pressure gradient imposed by the base flow. This pressure gradient can significantly affect the evolution of the turbine wake, such as the recovery of the wake center velocity deficit and the expansion of the wake. Most conventional wake modeling approaches, however, assume zero pressure gradient and a homogeneous base flow velocity. A practical approach to model wakes in topography, for instance, is to superpose the velocity deficit in the flat terrain on top of the topography. Although simple, this approach has been shown to work only for terrains with very gentle slopes [11,12]. Brogna et al. [13] proposed a modified form of the Gaussian model [4] to be used for their wind farm optimization study in topography. More recently, Farrell et al. [14] presented a wind farm wake model for varying base flow velocity field. They also based their wake model on the Gaussian model [4], while keeping the reference base flow velocity spatially variable. Hu et al. [15] presented a genetic algorithm based approach for siting wind turbines in complex terrain. To account for wake effects, they used an adapted Jensen model and Gaussian model based on the Brogna et al. [13] formulation. These approaches, however, do not explicitly account for the imposed pressure gradient, as the underlying models are derived under the assumption of a flat terrain. Recent years have seen an increased interest in data-driven approaches to the estimation of wake effects in wind farms on flat terrain (see e.g., [16–18]). On complex terrain, the problem complexity increases further due to the dependence of the flow characteristics (such as the imposed pressure gradients) on site-specific terrain characteristics. This hinders the applicability of data-driven modeling to complex terrains due to limitations related to available data for training purposes.

The only existing models that account for the effect of an imposed pressure gradient on wakes are the ones proposed by Shamsoddin and Porté-Agel [19,20] and in turn successfully applied by them to study the wake of a wind turbine sited upstream of a hill [21]. These models solve an ordinary differential equation (ODE) for the streamwise evolution of the maximum velocity deficit under pressure gradient, which is derived by applying streamwise momentum conservation in a control volume. A self-similar Gaussian profile of the wake velocity deficit is assumed, which has recently been verified by Dar et al. [22] and Dar and Porté-Agel [23] in different topographies. The invariance of the ratio between the maximum velocity deficit and wake width to the pressure gradient is used to close the system of equations, and to obtain the wake width under the pressure gradient situation. In order to obtain a numerical solution, a boundary condition is required to solve the ordinary differential equation for the streamwise evolution of the maximum velocity deficit. In their original work [19–21], the surrounding base flow imposes a zero pressure gradient at the turbine location and becomes non-zero from a certain location downstream of the turbine. Therefore, the maximum velocity deficit at the first streamwise position is assumed to be the same with or without the imposed pressure gradient. While true for the above-described scenario or for the situations where the imposed pressure gradient at the turbine location is small enough, the assumption may not be valid for situations where there is significant imposed pressure gradient at the turbine location. One such example is a wind turbine sited close to the edge of an escarpment, where the pressure gradient induced by the escarpment is high closer to the edge and vanishes as we move further away from it. Dar and Porté-Agel [23] applied the model of Shamsoddin and Porté-Agel [20] to predict the wake velocity deficit of a turbine sited close to the edge of an escarpment. They observed that the model worked well for the escarpments with a sloped or a smooth leading-edge, but its performance degraded with the increase in the sharpness of the escarpment's leading-edge.

The objective of the current work is to develop an analytical modeling framework that can be applied in situations where the turbine experiences an arbitrary pressure gradient imposed by the base flow. The new model develops on the one proposed by [20], where Bernoulli's equation is used to estimate a theoretical near-wake velocity under a non-zero imposed pressure gradient. This near-wake velocity is then used to obtain maximum wake velocity deficit at the start of the turbine far wake, where an ordinary differential equation is solved. The model is validated against the experimental data and compared with the results from two existing models [4,20]. The rest of the article is structured as follows: the analytical modeling framework is detailed in Section 2; validation of the model against experimental data and comparison with other models is performed in Section 3; finally, a summary of the work and concluding remarks are given in Section 4.

2. Analytical Modeling Framework

2.1. Problem Formulation

The mean streamwise velocity deficit in a wind turbine wake is known to show a self-similar Gaussian shape in the far wake in flat terrain [4], as well as in topography [22,23], and can therefore be expressed as:

$$\frac{U_b(x) - U_w(x,r)}{U_b(x)} = C(x)e^{-\left(\frac{r^2}{2\sigma(x)^2}\right)}, \tag{1}$$

where $U_b(x)$ is the velocity in the base flow (flow without turbine), $U_w(x,r)$ is the velocity in the wake flow, $C(x)$ is the normalized maximum velocity deficit at a certain streamwise location, $\sigma(x)$ is the wake width, x is the streamwise distance, and r is the radial distance from the wake center. For the sake of brevity, the term velocity is used to refer to mean streamwise velocity throughout the article, unless otherwise stated. Here, the wake velocity deficit is assumed to be axisymmetric around the wind turbine center. In situations where the velocity deficit is not perfectly axisymmetric, as stated by Shamsoddin and Porté-Agel [20], the problem is solved for an equivalent wake width expressed as a geometric mean of the lateral and vertical wake widths.

The base flow velocity $U_b(x)$ is only represented as a function of the streamwise distance, although in some situations it can also vary in other directions. For instance, in the case of two dimensional topography it can vary in both streamwise and vertical directions. Following Shamsoddin and Porté-Agel [21], the base flow velocity in the streamwise direction at the hub height of the turbine can be used as an approximation for $U_b(x)$. Alternatively, in the case of highly sheared or three-dimensional base flow, an averaged velocity within the rotor's projected area can be chosen to represent the base flow, although this approach would require more information on the base flow. The imposed pressure gradient is represented by the streamwise gradient of the base flow velocity, where $dU_b/dx = 0$ corresponds to the zero pressure gradient (ZPG), $dU_b/dx > 0$ indicates a favorable pressure gradient (FPG), and $dU_b/dx < 0$ represents an adverse pressure gradient (APG).

The objective of the current study is to present an analytical modeling framework that can predict the evolution of a wind turbine wake under an arbitrarily imposed pressure gradient, provided that the wake evolution under zero pressure gradient and the base flow under pressure gradient are known. The inputs for the zero pressure gradient wake evolution are the same as those required by the Gaussian model developed by Bastankhah and Porté-Agel, i.e., the turbine thrust coefficient and wake width [4].

2.2. Model Derivation

Following Shamdsoddin and Porté-Agel [20], the integral form of the streamwise momentum equation for an axisymmetric wind turbine wake under pressure gradient can be written as:

$$\frac{d}{dx}\int_0^\infty U_w(U_b - U_w)2\pi r dr + \int_0^\infty \frac{dU_b}{dx}(U_b - U_w)2\pi r dr = 0, \tag{2}$$

where the first term on the left-hand side represents the contribution of the turbine thrust, and the second term accounts for the effect of pressure gradient on the turbine wake. The term $(U_b - U_w)$ vanishes far from the wake center in a plane normal to the streamwise direction. In deriving the above equation, the continuity equation is used, and viscous effects are neglected. Moreover, the mean pressure gradient is represented by $U_b(dU_b/dx)$. Substituting Equation (1) into Equation (2) and replacing $\int_0^\infty exp(-r^2/2\sigma^2)2\pi r dr$ with $2\pi\sigma^2$ under the assumption of axisymmetry yields the following:

$$\frac{d}{dx}\left[2\pi U_b^2(x)\sigma^2(x)\left(C(x) - \frac{C^2(x)}{2}\right)\right] + \pi\frac{dU_b^2(x)}{dx}\sigma^2(x)C(x) = 0. \tag{3}$$

In the case of zero pressure gradient, the second term on the left-hand side of Equation (3) vanishes, and the following solution is obtained (see Bastankhah and Porté-Agel [4]):

$$C_0(x) = \frac{\Delta U_{max}(x)}{U_{b0}} = 1 - \sqrt{1 - \frac{C_T}{8(\frac{\sigma_0(x)}{D})^2}}, \tag{4}$$

where $C_0(x)$ is the normalized maximum velocity deficit under ZPG, ΔU_{max} is the maximum velocity deficit, U_{b0} is the reference base flow velocity under ZPG, C_T is the turbine thrust coefficient, $\sigma_0(x)$ is the wake width under ZPG, and D is the turbine rotor diameter. Once $C_0(x)$ is obtained, we can compute the invariant ratio between the maximum velocity deficit and wake width such as:

$$\lambda_0(x) = \lambda(x) = \frac{C_0(x)U_{b0}}{\sigma_0(x)}, \tag{5}$$

where λ_0 and λ are the ratios under zero and non-zero pressure gradients, respectively. The assumption of the invariance has been verified for different pressure gradient situations [19,20,24] and is used here to obtain the wake width under pressure gradient:

$$\sigma(x) = \frac{C(x)U_b(x)}{\lambda_0(x)}, \tag{6}$$

and to eventually solve Equation (3), which yields the following ordinary differential equation for $C(x)$ (as obtained by Shamsoddin and Porté-Agel [20]):

$$\frac{dC(x)}{dx} = \frac{-1}{\left(\frac{U_b^4(x)}{\lambda_0^2(x)}\right)(3C^2(x) - 2C^3(x))}\left[\frac{1}{4}\frac{dU_b^4(x)}{dx}\frac{C^3(x)}{\lambda_0^2(x)} + \left(C^3(x) - \frac{C^4(x)}{2}\right)\frac{d}{dx}\left(\frac{U_b^4(x)}{\lambda_0^2(x)}\right)\right]. \tag{7}$$

In order to obtain a numerical solution for $C(x)$ from Equation (7), a boundary condition is needed. In their original work, Shamsoddin and Porté-Agel [20] defined the boundary condition as:

$$C(x_i) = C_0(x_i), \tag{8}$$

which implies that at the starting point of the model (x_i), regarded as the start of the far wake (or alternatively the end of the near wake), the maximum velocity deficit is the same under a zero or non-zero pressure gradient. This assumption is valid in situations where the imposed pressure gradient is zero at the turbine location and becomes non-zero from a certain location in the far wake of the turbine. In fact, in their validation study [20] and application of the model to wake flows over hills [21], the pressure gradient by the terrain was imposed in the far wake, which resulted in the aforementioned boundary condition. However, if we consider a situation where the imposed pressure gradient at the turbine location or in its near wake is non-zero, the above-stated boundary condition does not hold.

Examples of such situations can be easily found, for instance, the wake of a turbine sited close to the edge of an escarpment and on top of a hill or a building.

In the following, we present a simplified theoretical estimation of the near wake velocity under a non-zero pressure gradient. Prior to that, it is useful to review some basic characteristics of the wind turbine's near wake. The flow in the near wake is greatly influenced by the turbine characteristics, and a common approach is to assume a gradual transition from a top-hat velocity distribution behind the rotor to a Gaussian distribution at the end of the near wake. This is due to the growth of the shear layer behind the rotor periphery, which expands radially with the increase in the streamwise distance, as the outer flow mixes with the wake flow. The wake center velocity is assumed to be theoretically constant in the near wake region, as the shear layer does not grow enough to re-energize the wake center in this region. Bernoulli's equation has been applied to the regions upstream and downstream of the turbine to estimate the near wake velocity for a wind turbine under uniform inflow and zero pressure gradient [5,25]. This theoretical near wake velocity has been used to estimate the end of the near wake and to provide a limit for the maximum velocity deficit obtained from an analytical model in various challenging scenarios, such as wind turbines in yawed conditions or the ones experiencing vertical wind veer [5,6]. It has also been implemented in different low-fidelity wake modeling utilities to estimate wake velocity at the start of the far wake (see e.g., [14]).

A schematic of the turbine wake is shown in Figure 1, where position 1 corresponds to an upstream location undisturbed by the turbine, position 2 is immediately in front of the rotor, position 3 is immediately behind the rotor, and position 4 corresponds to the location in the wake where the wake pressure becomes equal to the base flow pressure and there is no mixing between the outer (base) flow and wake flow. The conditions defined here for the application of Bernoulli's equation are similar to those used for actuator discs placed in a confined flow with a spatially heterogeneous base flow velocity [26,27]. Following [5,25], Bernoulli's equation for the control volumes up- and down-stream of the turbine can be written as:

$$\text{upstream: } P_{b1} + \frac{1}{2}\rho U_{b1}^2 = P_R^+ + \frac{1}{2}\rho U_R^2, \tag{9}$$

$$\text{downstream: } P_R^- + \frac{1}{2}\rho U_R^2 = P_{nw} + \frac{1}{2}\rho U_{nw}^2, \tag{10}$$

where P_{b1} is the base flow pressure upstream of the turbine (position 1 in Figure 1), and U_{b1} is the base flow velocity at the same location, the values of which can be obtained from the base flow information. Furthermore, P_R^+ and P_R^- are pressure values at the front and back sides of the rotor, and the velocities at these positions U_R are assumed to be the same. The wake center velocity in the near wake is U_{nw} (position 4 in Figure 1).

Subtracting Equations (9) and (10) result in:

$$[P_{b1} - P_{nw}] + \frac{1}{2}\rho[U_{b1}^2 - U_{nw}^2] - [P_R^+ - P_R^-] = 0, \tag{11}$$

where $[P_R^+ - P_R^-] = (1/2)\rho U_{bT}^2 C_T$, U_{bT} is the base flow velocity at the turbine location, and in the case of ZPG, $[P_{b1} - P_{nw}] = 0$. However, in the presence of a pressure gradient in the base flow, the later pressure difference can be obtained by applying Bernoulli's equation on the base flow between positions 1 and 4:

$$[P_{b1} - P_{nw}] = \frac{1}{2}\rho[U_{b4}^2 - U_{b1}^2], \tag{12}$$

where U_{b4} is the base flow velocity at position 4. After substituting the base flow pressure difference and pressure difference across the rotor in Equation (11), we obtain the following relation for U_{nw}:

$$U_{nw} = \sqrt{U_{b4}^2 - U_{bT}^2 C_T}. \tag{13}$$

In the case of ZPG, $U_{b1} = U_{bT} = U_{b4}$, and it can be easily shown that the above equation reduces back to the well known relation: $U_{nw}/U_{bT} = \sqrt{1 - C_T}$. Finally, the maximum velocity deficit for the boundary condition of Equation (7) can be written as:

$$C(x_i) = 1 - \frac{U_{nw}}{U_{bxi}}, \tag{14}$$

where U_{bxi} is the base flow velocity at the end of the near wake. In the case of a zero pressure gradient imposed by the base flow at the turbine location, the above equation reduces back to Equation (8).

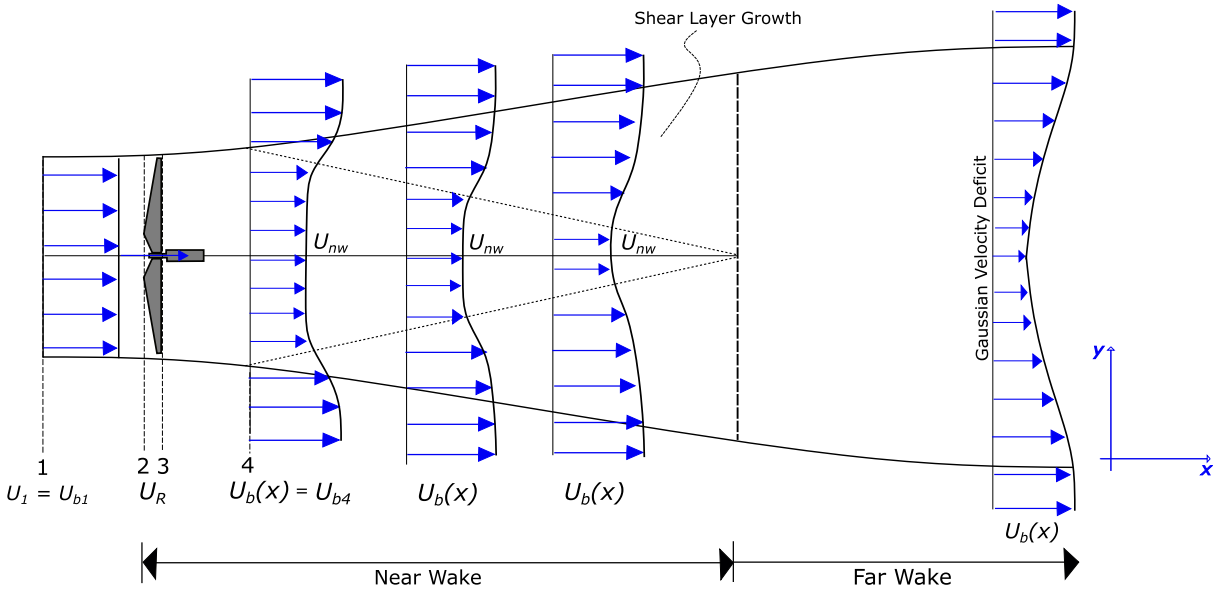

Figure 1. Schematic of a wind turbine wake.

3. Model Validation

Following the derivation, we aim to validate the model with experimental data. For this purpose, we use the experimental data from Dar and Porté-Agel [23]. In their experiments, a miniature wind turbine (WiRE-01) is placed one rotor diameter downstream of the edge of an escarpment, where the shape of the escarpment is varied between a forward-facing step with different edge curvatures and a ramp-shaped escarpment. Figure 2 shows the geometrical details of the escarpments used in the experiments, and the normalized base flow velocity at the turbine hub height. As can be seen, the variation in the base flow velocity is high closer to the turbine ($x/D = 0$, where D is the rotor diameter), and reaches almost a constant value about five rotor diameters downstream of the turbine. Different escarpment shapes also show differences in their base flow velocities, which indicates a difference in the imposed pressure gradient. The chosen experiments are well-suited to test the new model, as the imposed pressure gradient is higher closer to the edge of the escarpment (i.e., at the turbine location) and differs between the escarpments, which enables us to test the model under different pressure gradients. Table 1 presents a description of the escarpments.

In order to apply the pressure gradient model, we need two main inputs: the base flow velocity under the pressure gradient and the characteristics of the turbine wake under the zero pressure gradient ($C_0(x)$ and $\sigma_0(x)$). For the maximum velocity deficit under ZPG $C_0(x)$, we use Equation (4), which requires the turbine thrust coefficient C_T and wake width $\sigma_0(x)$. From experiments [23], the thrust coefficient of 0.8 is used, which does not change between the flat and escarpment cases [5,23]. To obtain the ZPG wake width, we use the linear growth of wake width in the far wake region [1]:

$$\frac{\sigma_0(x)}{D} = k_0 \frac{x}{D} + \epsilon, \tag{15}$$

where k_0 is the wake growth rate in ZPG, and ϵ is the initial wake width. The wake growth rate k_0 can be related to the streamwise turbulence intensity (TI) in the flow, where several linear relations between the streamwise turbulence intensity and the wake growth have been proposed in the literature [28,29]. Here, we use the relation proposed by Brugger et al. [29], which states $k_0 = 0.30 \times TI$, as it fits the wake growth rate found experimentally for the miniature wind turbine in flat terrain by Bastankhah and Porté-Agel [5]. As the pressure gradient model does not explicitly relate the turbulence intensity change in ZPG and PG conditions, we take the rotor-averaged turbulence intensity in the base flow at the turbine location to compute the wake growth rate for the ZPG wake. This is performed in order to account for the change in the turbulence intensity between the zero and non-zero pressure gradient situations. The theoretical normalized wake width ϵ value of $1/\sqrt{8}$ is used at the end of the near wake [5]. Following [5,30], the end of the near wake is assumed to be the position where the theoretical and experimental velocity deficit maximum on the escarpments become equal. The near wake length obtained by this criterion is very similar to the one obtained from theoretical relations derived for flat terrain [5,31].

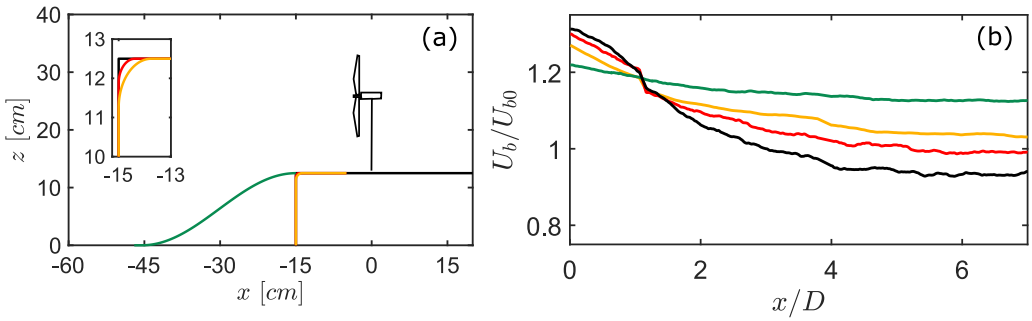

Figure 2. Side view of the escarpment geometry (**a**) and normalized base flow velocity at the hub height on top of the escarpments (**b**). Colors represent the respective escarpment shapes. The figure is adapted from Dar and Porté-Agel [23].

Table 1. Description of different validation cases and some key parameters.

Case	Description	U_h [ms^{-1}]	$k_0 = 0.3TI$	C_T	U_{b0} [ms^{-1}]
FFS-I	Sharp 90° Edge	4.7	0.0380	0.8	3.55
FFS-II	5% radius of curvature with respect to height	4.6	0.0290		
FFS-III	10% radius of curvature with respect to height	4.52	0.0231		
Ramp	33° maximum slope	4.34	0.0155		

In order to use Equation (13), we need to define position 4 in Figure 1. Mathematically speaking, this position should be chosen such that Equation (13) yields a real value. A choice of position 4 where Equation (13) results in an imaginary number would indicate a breakdown of the theory, which could be similar to the situation of actuator discs with thrust coefficients above 1 in the classical one-dimensional momentum theory [32]. Following [26,27], from a physical perspective, position 4 should correspond to a location where the pressure in the wake flow becomes equal to that in the base flow, and there is no mixing between the (outer) base and wake flow. Figure 3 shows the contours of the normalized turbulence kinetic energy in the turbine wake for different escarpment cases. Behind the turbine top tip level, a region of high turbulence kinetic energy can be observed, which is relatively thin closer to the turbine but starts to expand in the vertical direction from a certain position downstream, corresponding to the position where tip vortices start to breakdown and the outer flow starts to mix with the wake flow. Therefore, position 4 should be chosen before the region of high turbulence kinetic energy starts to expand in

the vertical direction. However, it should not be picked too close to the turbine to avoid influence of the pressure drop across the rotor.

A common approach in the literature [3,33,34] is to assume one rotor diameter downstream of the turbine as the distance where pressure in the wake and base flow equalizes. This position also lies within the region where the turbulence kinetic energy does not start to grow for all the cases. Therefore, we choose one rotor diameter downstream of the turbine as a common assumption for position 4 in all cases. It is to be noted that the choice of position 4 used here might not be universal, and future work should investigate this. The above discussion comes from the one-dimensional momentum theory for actuator discs, and in reality, the structure of the turbine near wake is much more complex. As shown by [5], the measured near-wake velocity deficit for the miniature turbine is higher than the theoretical one and varies instead of being a constant. This difference is attributed to several factors, including the wake of the nacelle and rotation of the wake. Although a simplified approximation, the theoretical near wake velocity provides useful information on the wake flow, such as the end of the near wake and a theoretical estimation for the velocity at the start of the far wake [5,14,30].

Once all the required inputs for the pressure gradient model have been obtained, we compute the maximum velocity deficit under pressure gradient using Equation (7) with the new boundary condition given by Equation (14) and wake width using Equation (6). In addition to the new model, we also test the pressure gradient model by Shamsoddin and Porté-Agel [20], and the Gaussian model by Bastankhah and Porté-Agel [4].

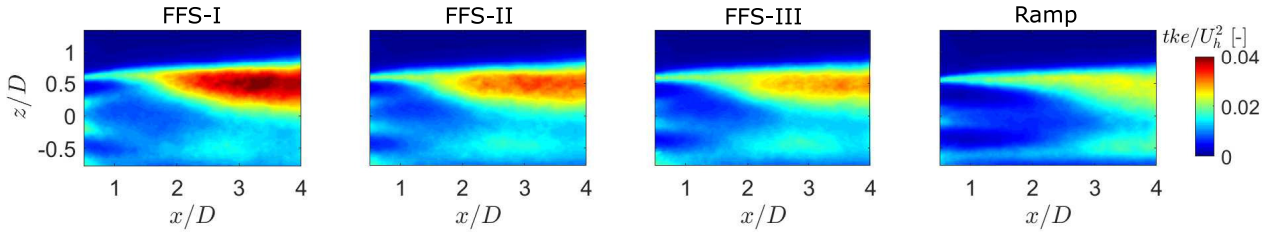

Figure 3. Contours of the normalized turbulence kinetic energy in the turbine wake.

A comparison of the maximum velocity deficit normalized by the hub height velocity between the experiments and the analytical models is shown in Figure 4 (left panels). The new pressure gradient model is represented by 'PG-New', whereas the pressure gradient model by Shamsoddin and Porté-Agel [20] is named 'PG-SPA', and the zero pressure gradient model (Gaussian model) by Bastankhah and Porté-Agel [4] is named 'ZPG'. The imposed pressure gradient depends on two factors: the shape of the escarpment, as a sharper edge would induce a higher pressure gradient, and the distance from the escarpment leading edge, as the pressure gradient would reduce with the increase in the distance from the escarpment edge. As a result, the differences between the different models compared here are also dependent on the same two factors. In general, the new pressure gradient model predicts the maximum velocity deficit reasonably well for all escarpments, as it accounts for the imposed pressure gradient at the turbine location. The PG-SPA model performs well for the ramp-shaped escarpment, as the imposed pressured gradient at the turbine location is lowest in this case. For the forward facing step cases, however, its performance degrades with the increase in the sharpness of the escarpment edge, where it works for the FFS-III case at distances greater than five rotor diameters, but underestimates the maximum velocity deficit for the other two FFS escarpments. This is due to the fact that the imposed pressure gradient is higher at the turbine location than in the far wake, and the PG-SPA model does not account for it, thereby underestimating the maximum velocity deficit. The zero pressure gradient model also underestimates the maximum velocity deficit for almost all the cases as it cannot account for the contribution of the pressure gradient to the velocity deficit.

The escarpments impose an adverse pressure gradient on the flow, which is known to slow down the recovery of the turbine wake compared to that under the zero pressure

gradient [20,24]. This explains why the models that do not account for the imposed pressure gradient at the turbine location underestimate the maximum velocity deficit. It can also be noted that for the two forward-facing step escarpments with relatively sharper edges (FFS-I and FFS-II), the PG-SPA and ZPG models show very similar values of the maximum velocity deficit. This is due to the fact that in the mentioned cases, the base flow velocity at the start of the far wake is almost the same with and without the escarpment. In other words, these escarpments not only induce the highest pressure gradient closer to the escarpment edge, but they also show the fastest decay in the induced pressure gradient with downstream distance. Therefore, at around four rotor diameters downstream of the turbine (five rotor diameters from the escarpment edge), the pressure gradient induced by the escarpments in the FFS-I and FFS-II cases is almost zero; as the PG-SPA model does not account for the imposed pressure gradient at the turbine location, it yields values similar to the ZPG model.

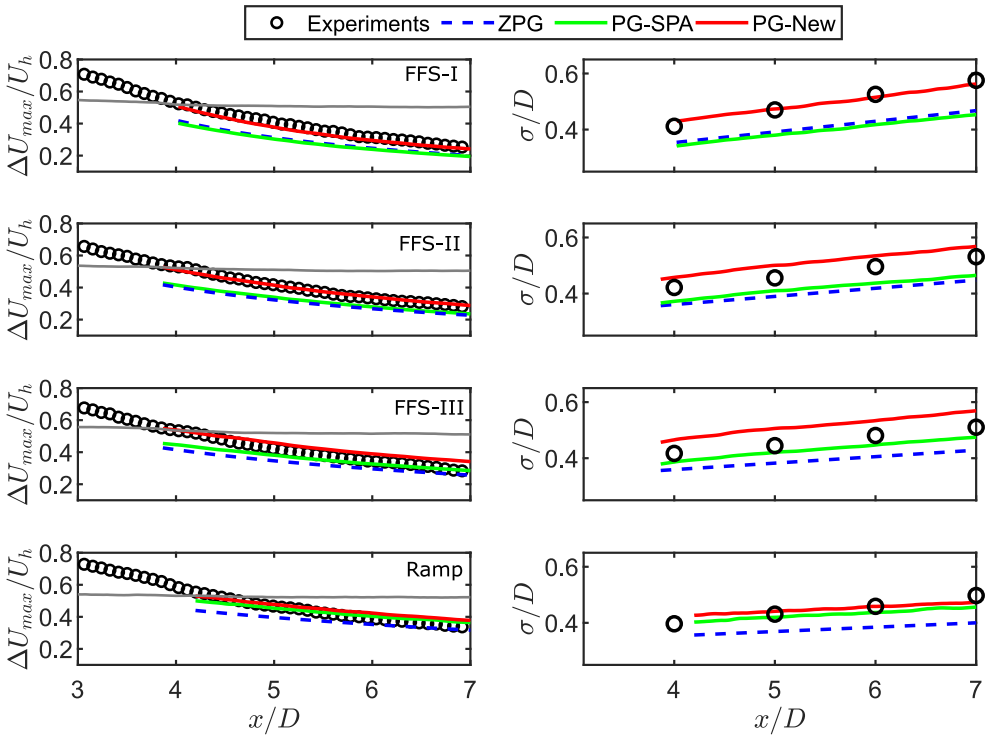

Figure 4. Comparison of the maximum normalized velocity deficit (**left**) and equivalent wake width (**right**) between the experiments and the analytical models. The solid gray line shows the theoretical maximum velocity deficit assuming a fixed near wake velocity.

Following the maximum velocity deficit, the equivalent wake width obtained from the analytical models is compared with the experimentally obtained one in Figure 4 (right panels). The ZPG wake width is smaller than the experimental equivalent wake width. This is to be expected, as an adverse pressure gradient results in a larger wake width compared to the zero pressure gradient one [20,24]. The PG-SPA underestimates the wake width for the FFS-I and FFS-II cases, but works well for the rest of the cases. The wake width obtained from the new pressure gradient model is observed to agree well with the experimental data for all the cases.

A comparison of the normalized velocity deficit profiles between the analytical models and experiments is shown in Figure 5. The velocity deficit profiles obtained from the new pressure gradient model are observed to agree well with the experimentally obtained profiles for all escarpment cases. As shown by Dar and Porté-Agel [23], the wake width in the lateral and vertical directions can vary depending on the escarpment shape. However, as mentioned earlier, in the current modeling approach, we solved the problem for an equivalent wake width ($\sigma = \sqrt{\sigma_y \sigma_z}$). Comparing the experimental and (new) analytical

velocity deficit profiles in the lateral and vertical direction shows that this approach works well. The PG-SPA and ZPG models, on the other hand, yield underestimated velocity deficit profiles for the most part. The PG-SPA model underestimates the velocity deficit profiles for the FFS-I and FFS-II cases, whereas it shows reasonable agreement for FFS-III case for downstream distances greater than five rotor diameters. For the ramp-shaped escarpment, it shows good agreement for all downstream distances. The ZPG model gives reasonable results at a downstream distance greater than five rotor diameters in the case of the ramp-shaped escarpment, which can be related to the fact that the effect of the pressure gradient is lowest for the ramp-shaped escarpment at high downstream distances. In general, we can say that the new pressure gradient model can successfully predict the velocity deficit in the turbine wake for all escarpment cases and outperforms the other two models tested in the study.

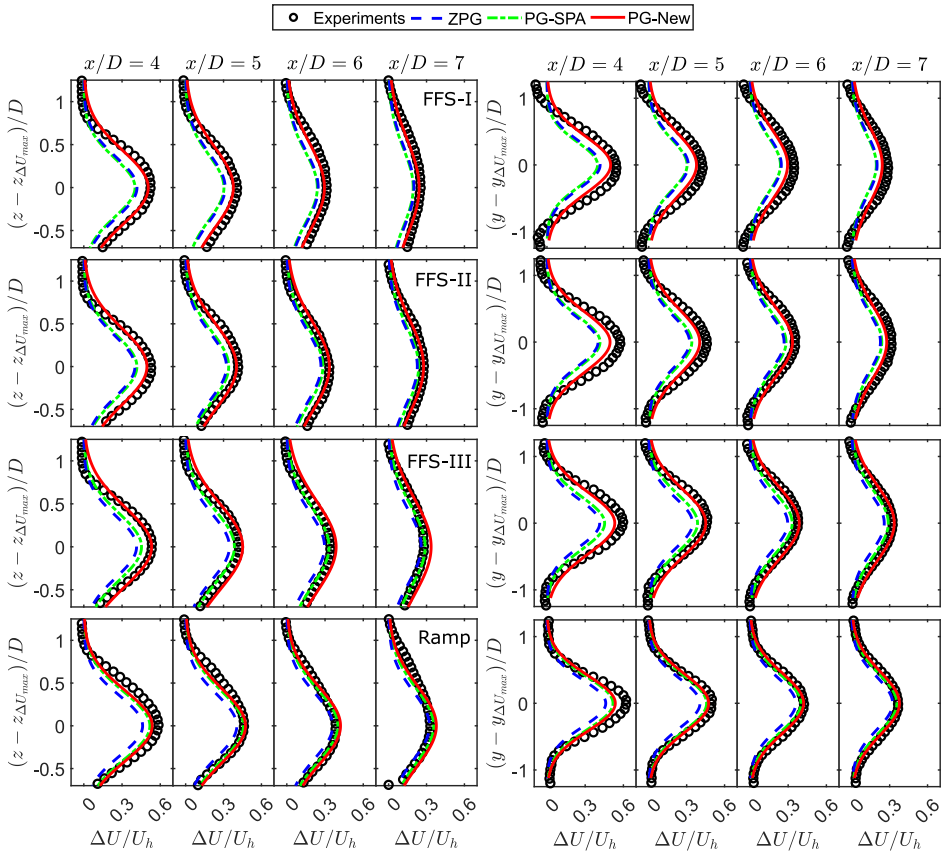

Figure 5. Comparison of the normalized vertical (**left**) and lateral (**right**) velocity deficit profiles between the experiments and the analytical models for different escarpments.

4. Concluding Remarks

Wind turbines sited in heterogeneous terrain experience varying levels of pressure gradient. In the current work, we have developed an analytical modeling framework that can predict the velocity deficit downstream of a wind turbine under an arbitrary imposed pressure gradient. The model is based on the cross-stream integration of the streamwise momentum conservation equation, and the self-similarity of the wind turbine wake velocity deficit. It solves an ordinary differential equation to estimate the maximum velocity deficit in the far wake, where a theoretical estimate of the near wake velocity under pressure gradient is used as a boundary condition. The current model builds on a previously proposed one, which only accounted for the effect of imposed pressure gradient in the turbine far wake. With the new model, we can also account for the effect of an imposed pressure gradient at the turbine location, which increases the number of applications the model can be used for. The pressure gradient model requires the base flow velocity under the pressure

gradient, and the wake characteristics (maximum velocity deficit and wake growth rate) under a zero pressure gradient as input parameters.

A validation of the new model against experimental data is performed. The experimental study involves a wind turbine placed close to the edge of escarpments of varying shapes. The turbine experiences varying levels of pressure gradient depending on the shape of the escarpment. The maximum velocity deficit and equivalent wake width obtained from the new model agree well with the experimental data for all cases. The velocity deficit profiles obtained analytically also show good agreement with both lateral and vertical velocity deficit profiles obtained experimentally. A comparison with another pressure gradient model and a model without any pressure gradient effects is also included. The new pressure gradient model is observed to outperform the other two models tested in the study for all cases. The other pressure gradient model worked for certain cases with relatively small imposed pressure gradients at the turbine location; however, its performance degraded for the cases with high imposed pressure gradients at the turbine location. Finally, the zero pressure gradient model only worked in the far wake of the escarpment with a smooth slope ahead of the turbine. Therefore, with the new modeling approach, we have extended the capability of analytical models to predict the wake velocity deficits of turbines experiencing an arbitrary imposed pressure gradient.

Author Contributions: Conceptualization, A.S.D. and F.P.-A.; methodology, A.S.D. and F.P.-A.; validation, A.S.D.; formal analysis, A.S.D.; investigation, A.S.D.; resources, F.P.-A.; data curation, A.S.D.; writing—original draft preparation, A.S.D.; writing—review and editing, F.P.-A.; supervision, F.P.-A.; funding acquisition, F.P.-A. All authors have read and agreed to the published version of the manuscript.

Funding: This research was funded by the Swiss National Science Foundation (grant number: 200021_172538) and the Swiss Federal Office of Energy (grant number: SI/502135-01).

Data Availability Statement: All data used in the study is contained within the article.

Conflicts of Interest: The authors declare no conflict of interest.

Nomenclature

U [ms^{-1}]	Time-averaged streamwise velocity
U_b [ms^{-1}]	Base flow velocity
U_w [ms^{-1}]	Wake flow velocity
C	Maximum normalized velocity deficit
r [m]	radial distance from turbine center
σ [m]	wake width
x [m]	streamwise distance/coordinate
z [m]	vertical distance/coordinate
y [m]	lateral distance/coordinate
λ [s^{-1}]	invariant ratio
C_T	thrust coefficient
k	wake growth rate
TI	rotor-averaged turbulence intensity
ΔU [ms^{-1}]	velocity deficit
D [m]	rotor diameter
subscripts	
0	zero-pressure gradient
b	base flow
w	wake flow
$1, 4, T$	position 1, 4, or turbine
nw	near wake
R	rotor
h	hub height
max	maximum

References

1. Porté-Agel, F.; Bastankhah, M.; Shamsoddin, S. Wind-turbine and wind-farm flows: A review. *Bound.-Layer Meteorol.* **2020**, *174*, 1–59. [CrossRef] [PubMed]
2. Jensen, N.O. *A Note on Wind Turbine Interaction*; Riso-M-2411; Risoe National Laboratory: Roskilde, Denmark, 1983; p. 16.
3. Frandsen, S.; Barthelmie, R.; Pryor, S.; Rathmann, O.; Larsen, S.; Højstrup, J.; Thøgersen, M. Analytical modelling of wind speed deficit in large offshore wind farms. *Wind. Energy Int. J. Prog. Appl. Wind. Power Convers. Technol.* **2006**, *9*, 39–53. [CrossRef]
4. Bastankhah, M.; Porté-Agel, F. A new analytical model for wind-turbine wakes. *Renew. Energy* **2014**, *70*, 116–123. [CrossRef]
5. Bastankhah, M.; Porté-Agel, F. Experimental and theoretical study of wind turbine wakes in yawed conditions. *J. Fluid Mech.* **2016**, *806*, 506. [CrossRef]
6. Abkar, M.; Sørensen, J.N.; Porté-Agel, F. An analytical model for the effect of vertical wind veer on wind turbine wakes. *Energies* **2018**, *11*, 1838. [CrossRef]
7. Shapiro, C.R.; Starke, G.M.; Meneveau, C.; Gayme, D.F. A wake modeling paradigm for wind farm design and control. *Energies* **2019**, *12*, 2956 . [CrossRef]
8. Ishihara, T.; Qian, G.W. A new Gaussian-based analytical wake model for wind turbines considering ambient turbulence intensities and thrust coefficient effects. *J. Wind. Eng. Ind. Aerodyn.* **2018**, *177*, 275–292. [CrossRef]
9. Lopez, D.; Kuo, J.; Li, N. A novel wake model for yawed wind turbines. *Energy* **2019**, *178*, 158–167. [CrossRef]
10. Li, L.; Huang, Z.; Ge, M.; Zhang, Q. A novel three-dimensional analytical model of the added streamwise turbulence intensity for wind-turbine wakes. *Energy* **2022**, *238*, 121806. [CrossRef]
11. Crespo, A.; Manuel, F.; Grau, J.C.; Hernández, J.; Garrad, A.D.; Palz, W.; Scheller, S. Modelization of wind farms in complex terrain. Application to the Monteahumada wind farm. In Proceedings of the European Community Wind Energy Conference 1993, Lübeck-Travemünde, Germany, 8–12 March 1993; pp. 440–443.
12. Hyvärinen A.; Segalini, A. Qualitative analysis of wind-turbine wakes over hilly terrain. *J. Phys. Conf. Ser.* **2017**, *854*, 012023. [CrossRef]
13. Brogna, R.; Feng, J.; Sørensen, J.N.; Shen, W.Z.; Porté-Agel, F. A new wake model and comparison of eight algorithms for layout optimization of wind farms in complex terrain. *Appl. Energy* **2020**, *259*, 114189. [CrossRef]
14. Farrell, A.; King, J.; Draxl, C.; Mudafort, R.; Hamilton, N.; Bay, C.J.; Fleming, P.; Simley, E. Design and analysis of a wake model for spatially heterogeneous flow. *Wind. Energy Sci.* **2021**, *6*, 737–758. [CrossRef]
15. Hu, W.; Yang, Q.; Chen, H.P.; Guo, K.; Zhou, T.; Liu, M.; Zhang J.; Yuan, Z. A novel approach for wind farm micro-siting in complex terrain based on an improved genetic algorithm. *Energy* **2022**, *251*, 123970. [CrossRef]
16. Nai-Zhi, G.; Ming-Ming, Z.; Bo, L. A data-driven analytical model for wind turbine wakes using machine learning method. *Energy Convers. Manag.* **2022**, *252*, 115130. [CrossRef]
17. Hwangbo, H.; Johnson, A.L.; Ding, Y. Spline model for wake effect analysis: Characteristics of a single wake and its impacts on wind turbine power generation. *IISE Trans.* **2018**, *50*, 112–125. [CrossRef]
18. Zehtabiyan-Rezaie, N.; Iosifidis A.; Abkar, M. Data-driven fluid mechanics of wind farms: A review. *J. Renew. Sustain. Energy* **2022**, *14*, 032703. [CrossRef]
19. Shamsoddin, S.; Porté-Agel, F. Turbulent planar wakes under pressure gradient conditions. *J. Fluid Mech.* **2017**, *830*, R4. [CrossRef]
20. Shamsoddin, S.; Porté-Agel, F. A model for the effect of pressure gradient on turbulent axisymmetric wakes. *J. Fluid Mech.* **2018**, *837*, R3. [CrossRef]
21. Shamsoddin, S.; Porté-Agel, F. Wind turbine wakes over hills. *J. Fluid Mech.* **2018**, *855*, 671–702. [CrossRef]
22. Dar, A.S.; Berg, J.; Troldborg, N.; Patton, E.G. On the self-similarity of wind turbine wakes in a complex terrain using large eddy simulation. *Wind. Energy Sci.* **2019**, *4*, 633–644. [CrossRef]
23. Dar A.S.; Porté-Agel, F. Wind-turbine wakes on escarpments: A wind-tunnel study. *Renew. Energy* **2022**, *181*, 1258–1275. [CrossRef]
24. Thomas, F.O.; Liu, X. An experimental investigation of symmetric and asymmetric turbulent wake development in pressure gradient. *Phys. Fluids* **2004**, *16*, 1725–1745. [CrossRef]
25. Manwell, J.F.; McGowan, J.G.; Rogers, A.L. *Wind Energy Explained: Theory, Design and Application*; John Wiley & Sons: Hoboken, NJ, USA, 2010.
26. Sørensen, J.N. *General Momentum Theory for Horizontal Axis Wind Turbines*; Springer: Berlin/Heidelberg, Germany, 2016.
27. Vogel, C.R.; Willden, R.H.J.; Houlsby, G.T. Blade element momentum theory for a tidal turbine. *Ocean. Eng.* **2018**, *169*, 215–226. [CrossRef]
28. Niayifar, A; Porté-Agel, F. Analytical modeling of wind farms: A new approach for power prediction. *Energies* **2016**, *9*, 741. [CrossRef]
29. Brugger, P.; Fuertes, F.C.; Vahidzadeh, M.; Markfort, C.D.; Porté-Agel, F. Characterization of wind turbine wakes with Nacelle-Mounted Doppler LiDARs and model validation in the presence of wind veer. *Remote. Sens.* **2019**, *11*, 2247. [CrossRef]
30. Vermeulen, P.E.J. An experimental analysis of wind turbine wakes. In Proceedings of the 3rd International Symposium on Wind Energy Systems, Copenhagen, Denmark, 26–29 August 1980; pp. 431–450.
31. Vahidi, D.; Porté-Agel, F. A physics-based model for wind turbine wake expansion in the atmospheric boundary layer. *J. Fluid Mech.* **2022**, *943*, A49. [CrossRef]
32. Hansen, M.O.L. *Aerodynamics of Wind Turbines*; Routledge: London, UK, 2015.

33. Crespo, A.; Hernandez, J.; Frandsen, S. Survey of modelling methods for wind turbine wakes and wind farms. *Wind. Energy Int. J. Prog. Appl. Wind. Power Convers. Technol.* **1999**, *2*, 1–24. [CrossRef]
34. Sanderse, B. *Aerodynamics of Wind Turbine Wakes-Literature Review*; Energy Research Center of the Netherlands: Sint Maartensvlotbrug, The Netherlands, 2009.